AD-A097 754 LASER DIODE LABS INC NEW BRUNSWICK NJ* F/G 20/5
RESEARCH AND DEVELOPMENT OF ADVANCED DESIGN INJECTION LASER DIO--ETC(U)
SEP 80 T E STOCKTON, F D SPEER DAAB07-77-C-2163
UNCLASSIFIED DELNV-77-C-2163 NL

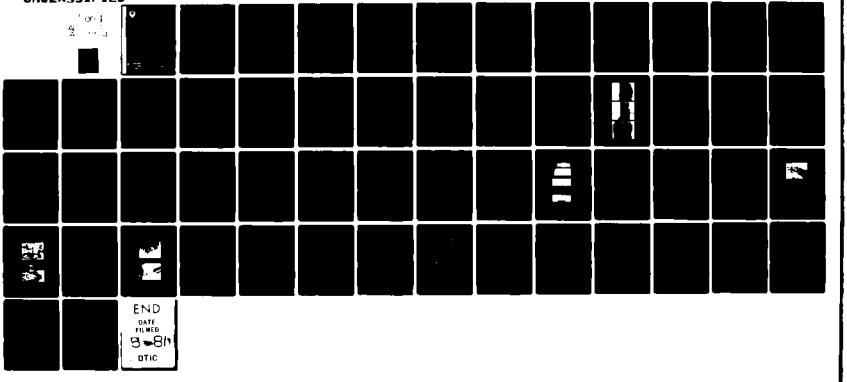

END
DATE FILMED
3-81
DTIC

RESEARCH AND DEVELOPMENT TECHNICAL REPORT
CORADCOM-DAAB07-77-C-2163

RESEARCH AND DEVELOPMENT OF ADVANCED DESIGN INJECTION LASER DIODES

THOMAS E. STOCKTON AND FRANK D. SPEER

LASER DIODE LABORATORIES
A M/A-COM COMPANY
1130 SOMERSET STREET
NEW BRUNSWICK, NEW JERSEY 08901

FINAL TECHNICAL REPORT
SEPTEMBER 30, 1980

CORADCOM
U S ARMY COMMUNICATIONS RESEARCH & DEVELOPMENT COMMAND
FORT MONMOUTH, NEW JERSEY 07703

Unclassified

SECURITY CLASSIFICATION OF THIS PAGE (When Data Entered)

REPORT DOCUMENTATION PAGE

READ INSTRUCTIONS BEFORE COMPLETING FORM

1. REPORT NUMBER: DELNV-77-C-2163	2. GOVT ACCESSION NO.: AD-A097754
3. RECIPIENT'S CATALOG NUMBER: -	
4. TITLE (and Subtitle): Research and Development of Advanced Design Injection Laser Diodes.	5. TYPE OF REPORT & PERIOD COVERED: Final Technical Report, Sep 78-9-78 through 9-80 Sep 80
	6. PERFORMING ORG. REPORT NUMBER: DELNV-77-C-2163
7. AUTHOR(s): Thomas E. Stockton and Frank D. Speer	8. CONTRACT OR GRANT NUMBER(s): DAAB07-77-C-2163
9. PERFORMING ORGANIZATION NAME AND ADDRESS: Laser Diode Laboratories, 1130 Somerset Street, New Brunswick, New Jersey 08901	10. PROGRAM ELEMENT, PROJECT, TASK AREA & WORK UNIT NUMBERS: -
11. CONTROLLING OFFICE NAME AND ADDRESS: U.S. Army Electronics R & D Command, Night Vision, Electro-Optics Laboratory, Fort Belvoir, Virginia 22060	12. REPORT DATE: 30 Sep 80
	13. NUMBER OF PAGES: 48
14. MONITORING AGENCY NAME & ADDRESS (if different from Controlling Office): Night Vision, Electro-Optics Laboratory, Laser Division, Attn: DELNV-L (Mark Skeldon), Fort Belvoir, Virginia 22060	15. SECURITY CLASS. (of this report): Unclassified
	15a. DECLASSIFICATION/DOWNGRADING SCHEDULE: N/A

16. DISTRIBUTION STATEMENT (of this Report)

Approved for public release; distribution unlimited.

17. DISTRIBUTION STATEMENT (of the abstract entered in Block 20, if different from Report)

-

18. SUPPLEMENTARY NOTES

-

19. KEY WORDS (Continue on reverse side if necessary and identify by block number)

Liquid Phase Epitaxy
GaInAsP Laser Diode
Quaternary Laser Diode
Injection Laser
Long Wavelength Laser Diode

20. ABSTRACT (Continue on reverse side if necessary and identify by block number)

High peak power, pulsed GaInAsP/InP Large Optical Cavity (LOC) injection lasers emitting in the 1.0 to 1.3 micron region have been developed and studied under this program. This final report describes efforts directed toward the optimization of these devices and, in particular, concentrates on the following points:

i. Materials and structure development required to extend wavelength and peak power capability.

DD FORM 1 JAN 73 1473 EDITION OF 1 NOV 65 IS OBSOLETE

405626

Unclassified

SECURITY CLASSIFICATION OF THIS PAGE (When Data Entered)

ii. Process development connected with the fabrication of high power stripe geometry long wavelength lasers.
iii. Package development and fiber coupling techniques for these devices.

Excellent peak power performance, on the order of 4mW per micron of junction length, was obtained for quaternary LOC laser diodes at a peak wavelength of 1.16 microns. In addition, greater than 25% coupling efficiency was demonstrated for 3 mil stripe quaternary LOC lasers coupled to 55 micron core graded index fiber. Peak optical power in excess of 75 mW was routinely obtained from the fiber pigtail. These devices are extremely well suited as sources for long haul, low bandwidth digital fiber optic systems where their high peak power capability can compensate for fiber darkening in high level radiation environments.

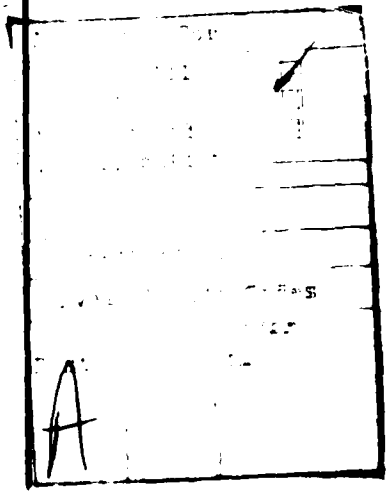

ABSTRACT

High peak power, pulsed GaInAsP/InP Large Optical Cavity (LOC) injection lasers emitting in the 1.0 to 1.3 micron region have been developed and studied under this program. This final report describes efforts directed toward the optimization of these devices and, in particular, concentrates on the following points:

i. Materials and structure development required to extend wavelength and peak power capability.

ii. Process development connected with the fabrication of high power stripe geometry long wavelength lasers.

iii. Package development and fiber coupling techniques for these devices.

Excellent peak power performance, on the order of 4 mW per micron of junction length, was obtained for quaternary LOC laser diodes at a peak wavelength of 1.16 microns. In addition, greater than 25% coupling efficiency was demonstrated for 3 mil stripe quaternary LOC lasers coupled to 55 micron core graded index fiber. Peak optical power in excess of 75 mW was routinely obtained from the fiber pigtail. These devices are extremely well suited as sources for long haul, low bandwidth digital fiber optic systems where their high peak power capability can compensate for fiber darkening in high level radiation environments.

TABLE OF CONTENTS

LIST OF FIGURES

1.0 Introduction

The primary objective of this program was the development of high peak power injection laser sources in 1.0 to 1.3 micron wavelength region. Ultimately, these devices should be suitable for extended range (>50Km) fiber optic data transmission at data rates in excess of 10 Megabits/second. With this in mind, a secondary objective of the program involved the investigation of various techniques for optimization of coupling efficiency between the laser diode and optical fiber.

This report describes efforts directed toward the optimization of fiber coupled long wavelength pulsed lasers and, in particular, concentrates on the following topics:

a. Materials and Structure Development required to extend both wavelength and peak power range of longwave ILDs.

b. Process Development required for the fabrication of high power stripe geometry longwave ILDs.

c. Package Development and Fiber Coupling Techniques aimed at maximizing launched power in multimode graded index optical fiber.

d. Device performance including threshold, DQE, wavelength, and reliability optimization.

2.0 Background

The 1.0-1.3 μm wavelength range is of particular interest for optical fiber communications because silica fibers have minimum attenuation and the material dispersion reaches zero in this range. Also, optical fibers appear to be more radiation resistant at wavelengths longer than 0.9 μm.

For diode lasers in the 1.0-1.3 μm region, the multiheterostructure GaInAsP/InP system offers major advantages over other candidate semiconductor materials. By adjusting its composition, GaInAsP can be lattice matched to InP for a wide range of wavelength values from 0.95 μm to 1.7 μm without the need for graded composition layers.

In Figure 1, the room temperature bandgap and corresponding wavelength of alloys in the $Ga_{1-x}In_xAs_{1-y}P_y$ system are plotted against the lattice constant. The position of the dashed vertical line lying within the shaded area represents GaInAsP alloys that have the same lattice constant as InP. Since InP has a higher energy gap and a lower refractive index than any of these alloys, both carrier and optical confinement can be achieved by sandwiching the GaInAsP active layer between two InP layers.

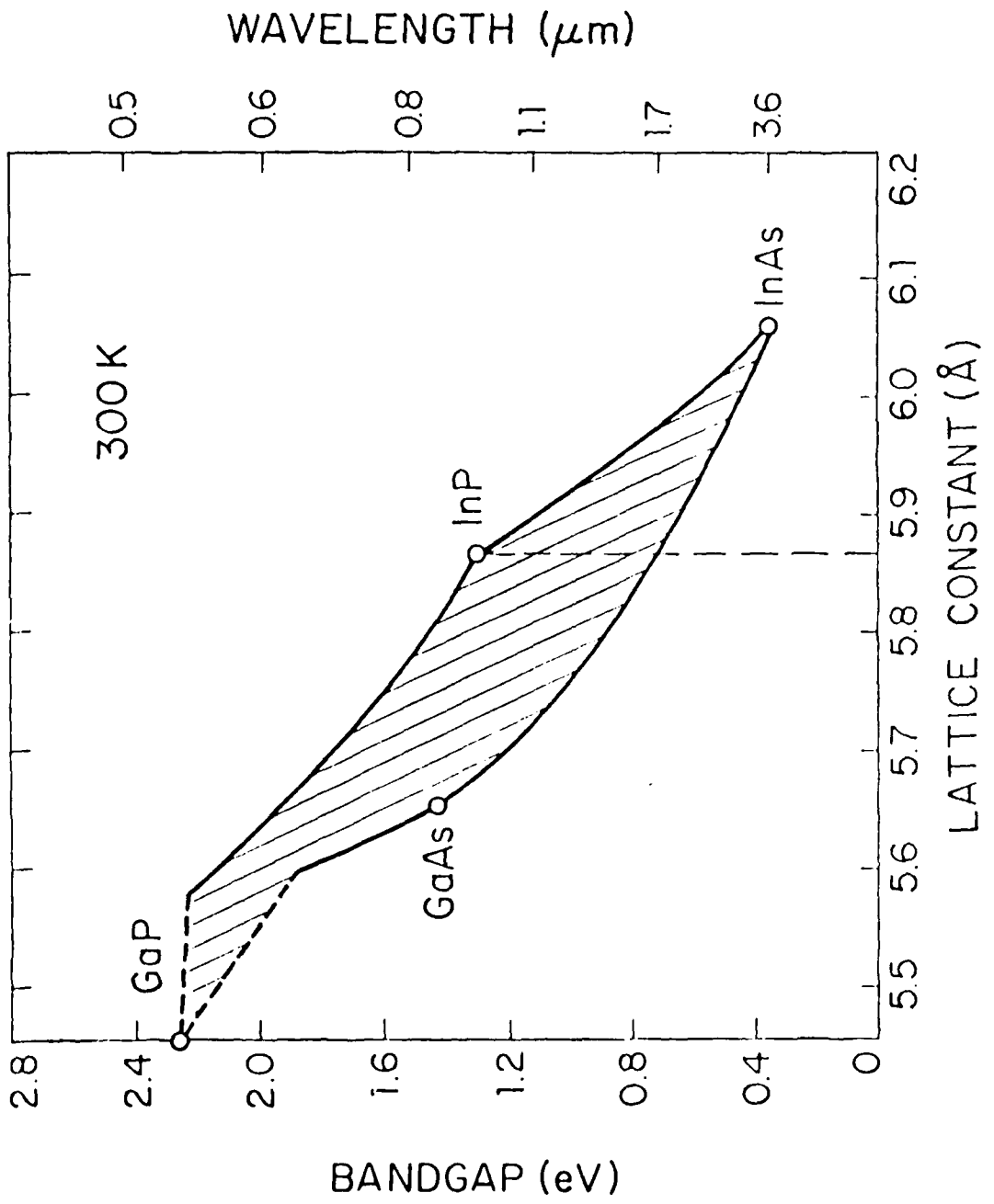

Figure 1. Wavelength, Bandgap vs. Lattice Constant

The conventional DH GaInAsP/InP laser consists of a thin GaInAsP layer and two InP confining layers. Usually, the GaInAsP active layer is only 0.2 to 0.3 μm thick in order to provide the low threshold current density required for CW operation at room temperature. The structure described above can exhibit low catastrophic damage limit, however, and large beam divergence due to its small emitting area and thin recombination region. In order to increase the maximum peak output power as well as reduce the beam divergence, thicker active regions as well as wide stripe contacts are required. Early on in this program, two types of LOC (large optical cavity) structures were investigated.

The epitaxial structure, bandgap profile, and index of refraction profile for Type I laser are shown in Figure 2. It consists of four LPE layers, namely: n-InP, n-$Ga_xIn_{1-x}As_yP_{1-y}$, p-$Ga_xIn_{1-x}As_yP_{1-y}$, and p-InP, which are grown successively on an InP substrate. Carrier confinement is provided by barriers at the p-InP/p-$Ga_xIn_{1-x}As_yP_{1-y}$ interface and also the p-$Ga_xIn_{1-x}As_yP_{1-y}$/n-$Ga_xIn_{1-x}As_yP_{1-y}$ P/N junction. Optical confinement is provided by the two heterojunctions between the InP and GaInAsP materials.

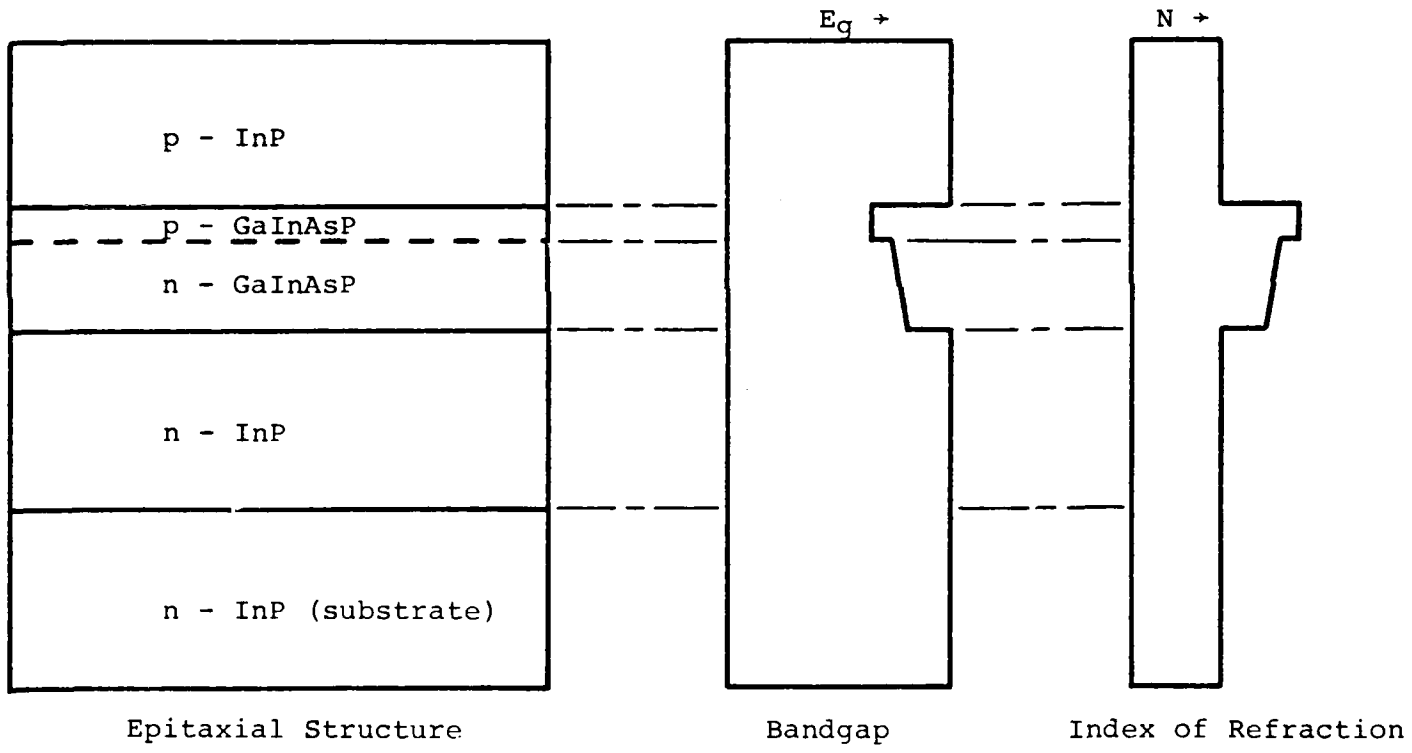

Figure 2. Type I LOC

The Type I LOC laser is suitable for 1.1-1.3 μm wavelength region but, as the energy bandgap and index of refraction of the GaInAsP approach that of the InP (which occurs for the emission wavelength in the 1.06 μm region), both carrier and optical confinement become too weak to obtain low threshold current or high quantum efficiency. The Type II LOC laser was investigated in an attempt to eliminate these potential problems by using a new concept in material design. The basic scheme is similar to that of Type I LOC laser except that the two InP confining lasers are replaced with two AlGaInAsP lasers. The incorporation of Al in GaInAsP has several advantages: The energy bandgap for AlGaInAsP is larger than that of GaInAsP and therefore provides the necessary carrier and optical confinement. Since the lattice constant for the Ga- and Al- containing III-V compounds are very close in value (e.g., a_o = 5.653Å for GaAs and 5.661Å for AlAs; a_o = 5.451Å for GaP and 5.462Å for AlP) the substitution of Al for Ga in GaInAsP can be made without significantly changing the lattice constant of the resulting material.

The epitaxial structure, bandgap and index of refraction for Type II laser is illustrated in Figure 3.

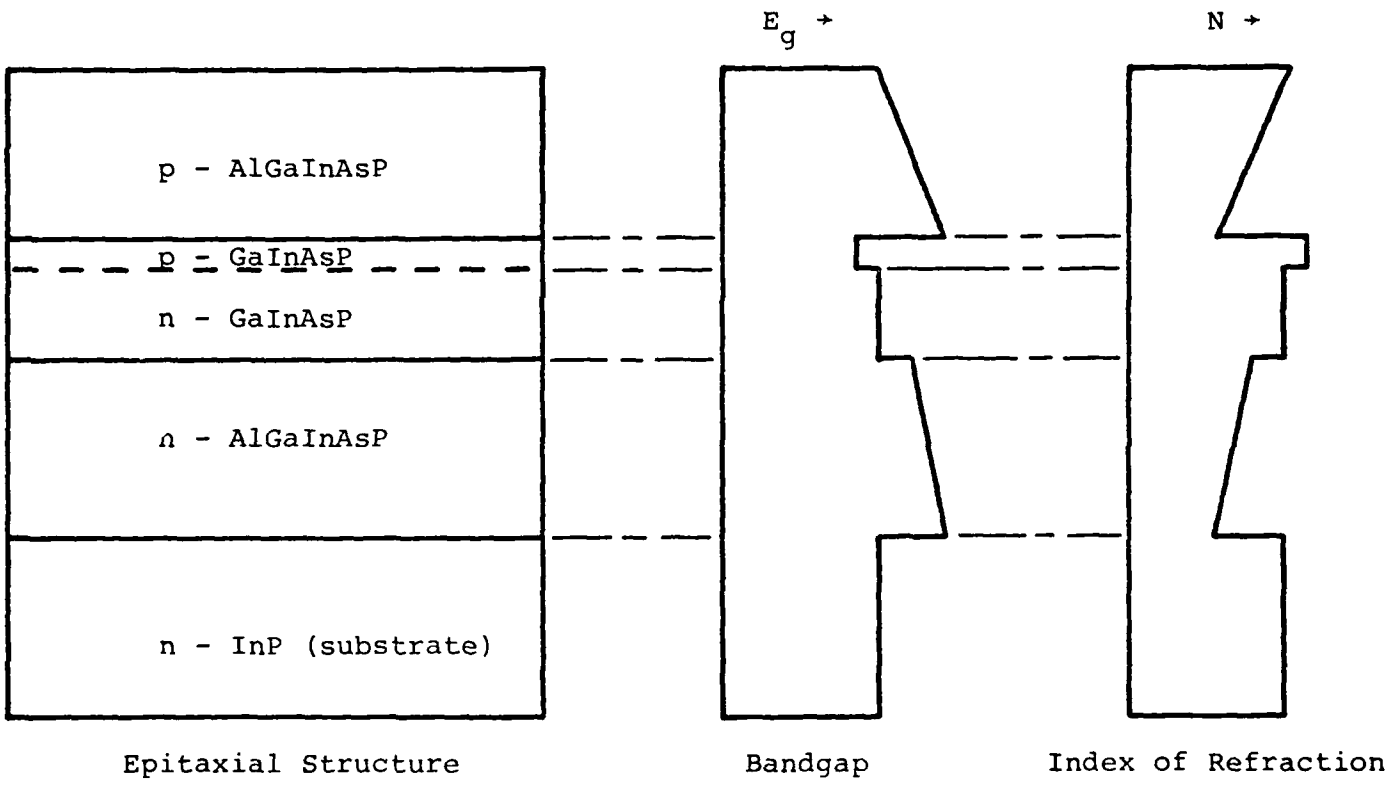

Figure 3. Type II LOC

It should be noted that exploratory work performed during the initial phase of this program in the quinternary AlGaInAsP system is believed to be first attempt to synthesize and epitaxially deposit this compound.

3.0 Materials and Structure Development

3.1 AlGaInAsP Experiments

During the first quarter, several single layer LPE runs were made in an attempt to determine whether or not Aluminum could be successfully incorporated in the quaternary melt. The growth temperature in these experiments was 635°C. In general, for all melt concentrations employed, surface morphology of the grown layer was poor with severe substrate non-wetting observed for higher Aluminum concentrations. It was determined that for Aluminum melt concentrations above 0.15 atomic percent, satisfactory epitaxy could not be obtained under any circumstances. Alternatively, if the melt concentration of Aluminum remained below 0.035 atomic percent, it was possible to obtain epitaxial layers which, although generally poor, exhibited no visible misfit crosshatch. A simple double heterostructure was designed to determine whether or not this acceptable limit of Aluminum was sufficient to generate the ΔEg and Δn discontinuities required for room temperature lasing. The test structure consisted of four compositionally similar quaternary layers; however, the first and third

melts contained Aluminum thus forming an optical waveguide. Doping was appropriately adjusted in the conventional manner so that the P/N junction was located within the second quaternary layer (active region).

Although several runs of this type were successfully synthesized, none exhibited lasing characteristics even at current densities in excess of 20KA/cm^2. For this reason, exploratory efforts in the quinternary AlGaInAsP system were abandoned in favor of the more conventional InP/GaInAsP LOC structure. It should be noted, however, that further analytical study, beyond the scope of the device effort performed under this contract, is required to adequately characterize the quinternary.

3.2 InP/GaInAsP LOC Development

During the remainder of the program, development effort concentrated on the Type I LOC structure described previously. Because maximum launched peak power into 50 μm core fiber was a desired program objective, a 3 mil stripe geometry LOC was found to be a suitable structure for optimization. The basic design, a selectively diffused, nitride isolated stripe geometry LOC, is shown in Figure 4. In this device, a simple wide cavity (>0.4 μm) double heterostructure is grown with an unintentionally doped n-type quaternary active region (2). Careful adjustment of the p-type dopant (Zinc) in the InP cladding layer (3) leads to an outdiffusion of zinc into the active region during LPE growth. Optimum device performance of the LOC structure is obtained when the P/N junction is located symmetrically within the active layer. Stripe geometry is formed by selective diffusion of Zinc through a silicon nitride mask so that the n-type quaternary blocking layer (4) is converted to p-type along the length of the stripe. Unlike analogous devices in GaAlAs, in which the active region thickness is optimum around 2.0 μm,

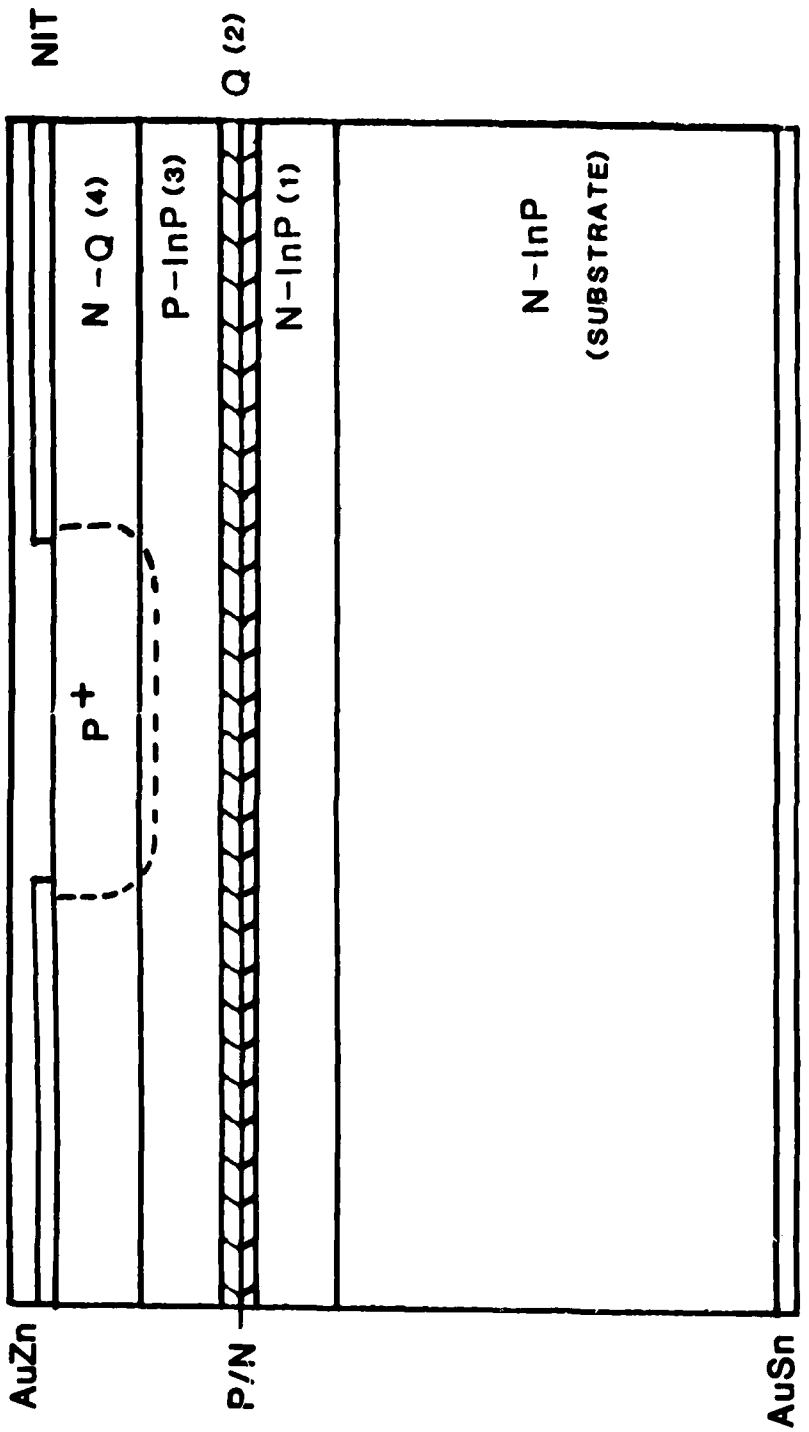

Figure 4 GaInAsP/InP LOC Structure

acceptable performance could only be obtained for $d \gtrsim 0.5$ μm. This is most likely a result of reduced carrier confinement which accompanies the smaller bandgap step between InP and GaInAsP. In addition, the minimum peak wavelength for which acceptable threshold and quantum efficiency could be obtained was 1.15 microns. This corresponds to the solid composition quaternary $Ga_{0.16}In_{0.84}As_{0.23}P_{0.77}$. Considerable difficulty in obtaining high quality lattice matched quaternary layers was encountered in attempting to grow shorter wavelength devices (<1.1 μm). It therefore remains uncertain whether there is any fundamental limitation to operation at shorter wavelengths using the LPE quaternary or this result is simply due to the inability to obtain proper melt compositions.

During the course of the program, peak power performance was optimized for $\lambda p = 1.16$ μm. Melt compositions for this structure are summarized in Figure 5.

InP LPE RUN SHEET

Run # RQ-111 Crystal # InP(215-R1) Furnace/Boat 3/RD3-A

Date 12-27-79 Slice/Thickness 12.8 mil Operator A.M.

Run	In gm	InP mg	InAs mg	GaAs mg	Dopants mg	Growth Period	Temp. °C	Layer Thickness µm
1	6	25.08	X	X	X	5 Sec	635°	Etch Melt
2	6	56.11	X	X	6.02 Te 400.08 Sn	5.5°	634.7°	
3	6	39.58	301.98	38.07	X	90 Sec	629.2°	0.45
4	6	55.98	X	X	5.04 Zn	4.0°	628.6°	2.11
5	6	39.65	302.02	38.10	X	3.0°	624.6°	1.05
6						Thru	621.6°	

Vacuum: 20 µ Flow Rate: 130 cc Flush Time: 60 min. Saturate: 90 min.

Start: 650°C Rate: 15°C/hr. Grow: 635°C

Comments:

Figure 5. Quaternary Melt Compositions for 1.16 µm LOC Structure

The substrate material used in these experiments was <100> oriented InP single crystal, Sn doped to a carrier concentration of $2X10^{18}cm^{-3}$ having a dislocation density of $<7X10^{4}cm^{-2}$. Wafers, 15 mil thick, were sliced from the InP ingots and each wafer cut into four $(1.2\ cm)^2$ substrates.

Each substrate was lapped with 2 μm alumina powder to remove any surface damage and polished to a mirror-like finish with a chemical-mechanical 1% Bromine-Methanol solution. Both MRC and Sumitomo material was utilized but no significant differences in substrate quality or resulting LPE could be ascertained. Unlike GaAs substrate, high quality, low dislocation InP crystal has not been readily available until very recently.

Conventional slider boat LPE was used to generate high quality epitaxial wafers. Excellent morphology and layer thickness control was obtained using an under-saturated Indium etch melt to eliminate the effects of substrate dissociation during saturation. Saturation was performed at 650°C for 90 minutes and growth of the first layer was initiated at 635°C using a constant cooling rate of 15°C/hour. In the single phase technique used here, melts are precisely formulated so

that they are just saturated at the growth temperature of their respective layers.

Figure 6 shows a stained cross section of the quaternary LOC wafer (RQ-111) used to fabricate devices delivered under this contract. The three SEM photographs, Figures 6a, b, and c, are taken from the lead, center, and trailing regions of the epi wafer respectively and span a distance of approximately 9 millimeters. Uniformity of the layers is excellent for the InP/GaInAsP material system but not as good as can be obtained with the two phase/source wafer technique commonly employed for GaAlAs ternary structures. Figure 7 outlines the actual dimensions for each of the sampling points. (The vertical 1 centimeter marker in Figure 6 equals 1 micron; also, the first cladding layer - substrate interface is not visible). Taper in the active region (2) is approximately 16% across the surface of the epi wafer; whereas, the thicker layers (3, 4) show approximately 8% and 14% taper respectively. Figure 6b also shows an EBIC (electron beam induced current) trace superimposed on the epilayer micrograph. The diffused P/N junction is not visible within the active region

Figure 6. SEM Micrographs of RQ-111 (10KX)

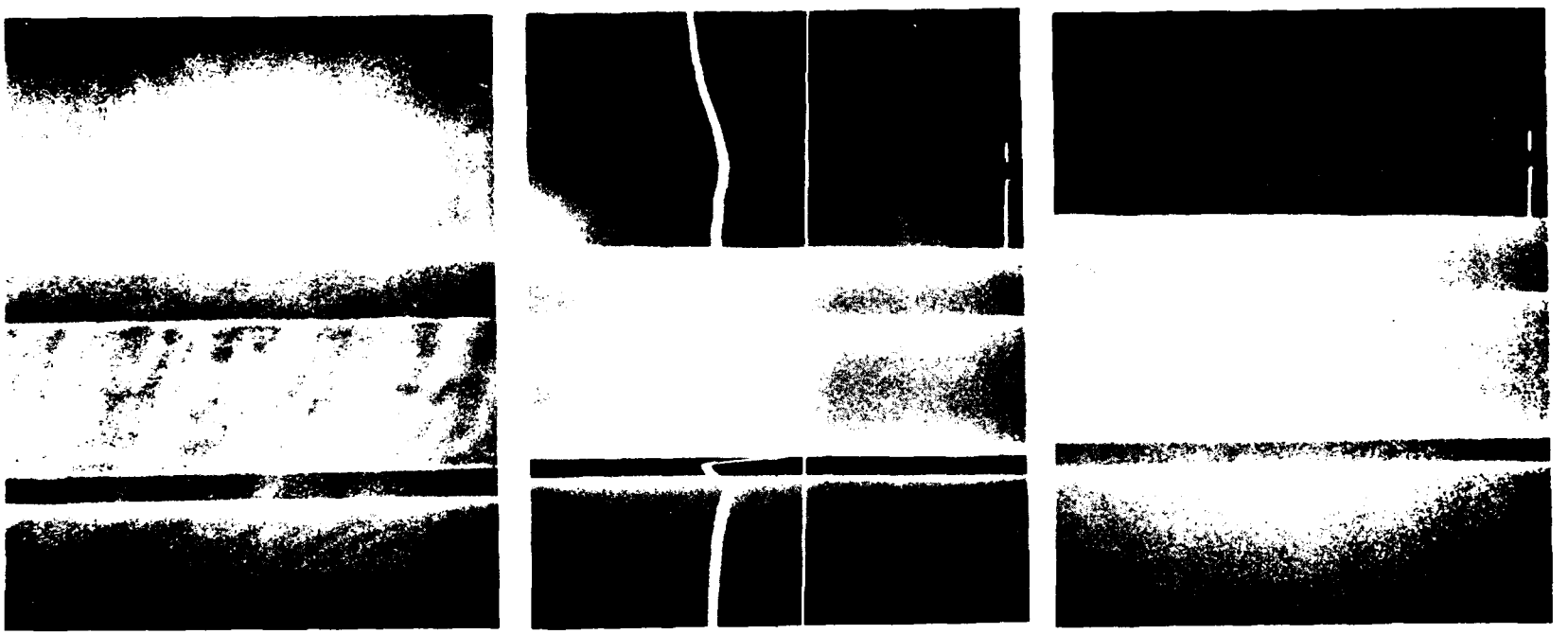

a. Lead

b. Center w/EBIC Scan

c. Trail

Sample # RQ - 111 Date: 1-3-80

Structure:

Type of Micrograph Required: SE [X]

AE/EBIC-LS [ ] Magnification

Thickness: SE [X] 10KX

LAYER	LEFT	CENTER	RIGHT	AVERAGE
1. I (Clad)	-	-	-	~ 3
2. Q(Active)	0.48	0.41	0.45	0.45
3. I (Clad)	2.23	2.05	2.06	2.11
4. Q (Cap)	0.97	1.05	1.12	1.05
5.				
6.				
7.				
8.				

REMARKS: Etched in 6:1:1, H_2SO_4: H_2O_2: H_2O for 50 Seconds to delineate junction.

Figure 7. Layer Thicknesses for Quaternary LOC Structure

since the particular etch used to delineate layer interfaces is not sensitive to doping type. The EBIC trace, however, clearly shows the location of the P/N junction centered within the quaternary active layer. (The P/N junction is indicated by the EBIC peak in layer 2).

The Type I quaternary LOC structure grown in accordance with the melt formulations given in Figure 5 has yielded reproducibly good pulsed laser performance chsracteristics at 1.16 μm and efforts to extend the wavelength range to 1.3 microns have met with some success. Details of stripe geometry laser fabrication and device performance are given in the following sections.

4.0 Wafer Processing for Fabrication of Stripe Geometry Quaternary LOC Structures

Figure 8 (a through i) describes the wafer processing sequence required for the fabrication of stripe geometry quaternary LOC lasers. As shown in Figure 8a, the structure consists of 4 layers epitaxially deposited on <100> InP substrate as follows:

1. n-type InP cladding layer ~3.0 μm
2. GaInAsP active layer 0.5 μm
   containing the diffused P/N junction
3. p-type InP cladding layer 2.0 μm
4. n-type GaInAsP cap layer 1.0 μm

Stripe geometry is defined by selective diffusion of zinc through the cap layer.

Diffusion masking is achieved through the use of a Si_3N_4 layer deposited by chemical vapor deposition (CVD) on the surface of the epitaxial wafer. Stripes are subsequently etched through the Si_2N_4 layer via standard photolithographic and plasma etching techniques. Selective Zn diffusion is carried out at 550°C in a semi-sealed ampoule system. The wafer is then backlapped to 75 μm and contacts are vacuum deposited; Au/Sn on the p-and n-sides respectively. The following paragraphs briefly describe the primary processes outlined in Figure 8.

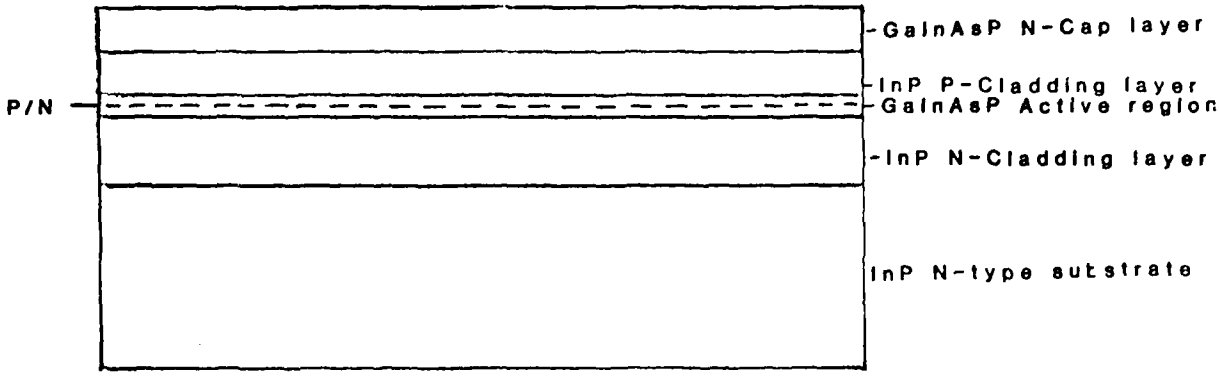

Fig. 8a GaInAsP/InP Laser structure

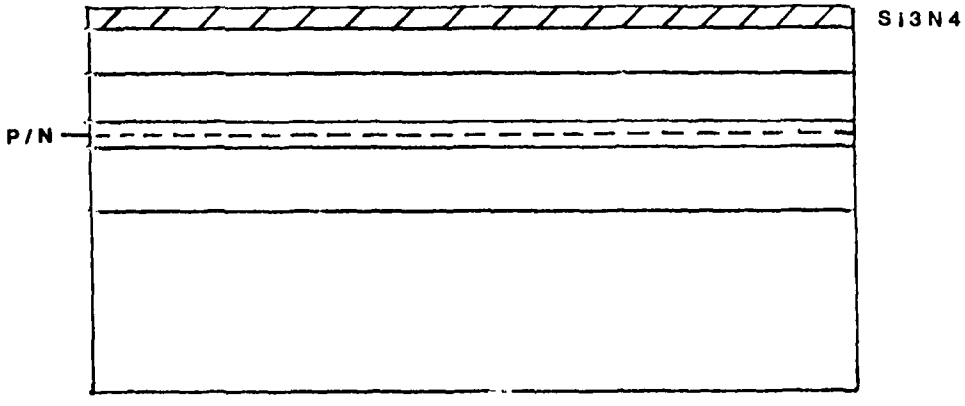

Fig. 8b Laser structure W/Si3N4 mask

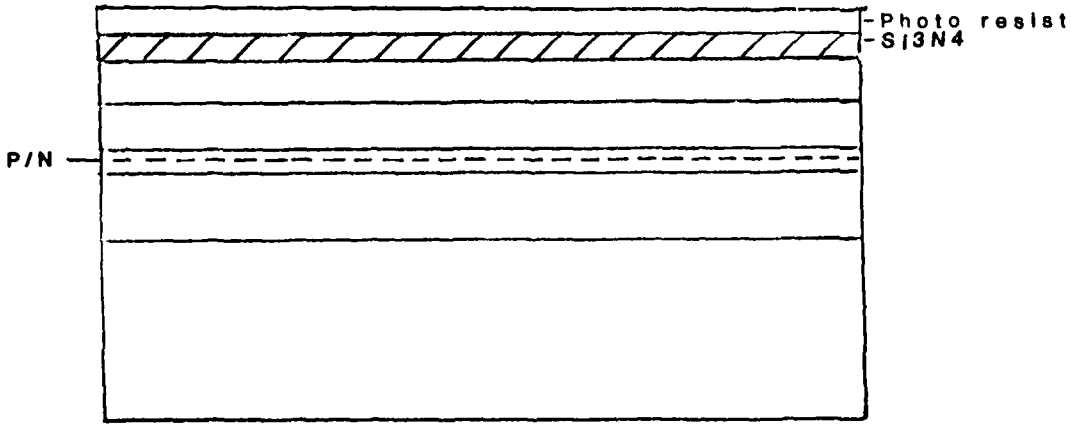

Fig.8c Photo resist mask

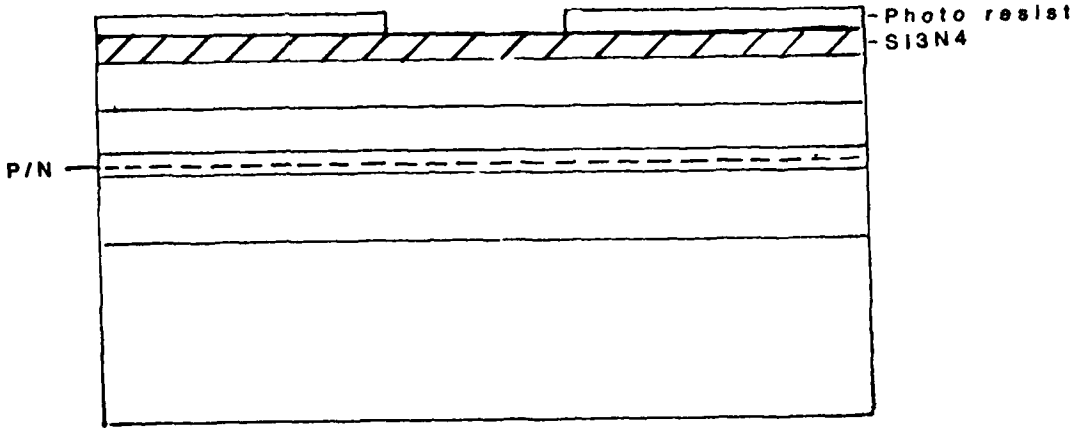

Fig. 8d Exposed window thru the photo mask

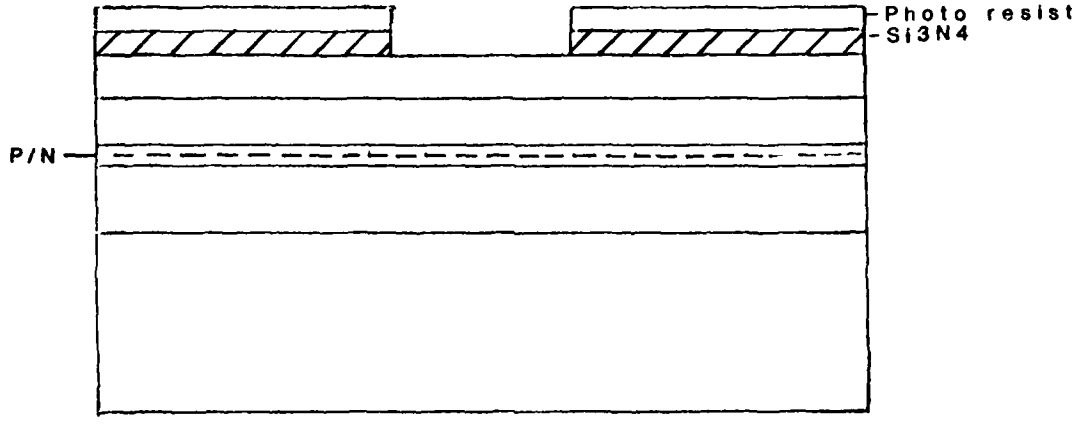

Fig. 8e Selective removal of the Si3N4

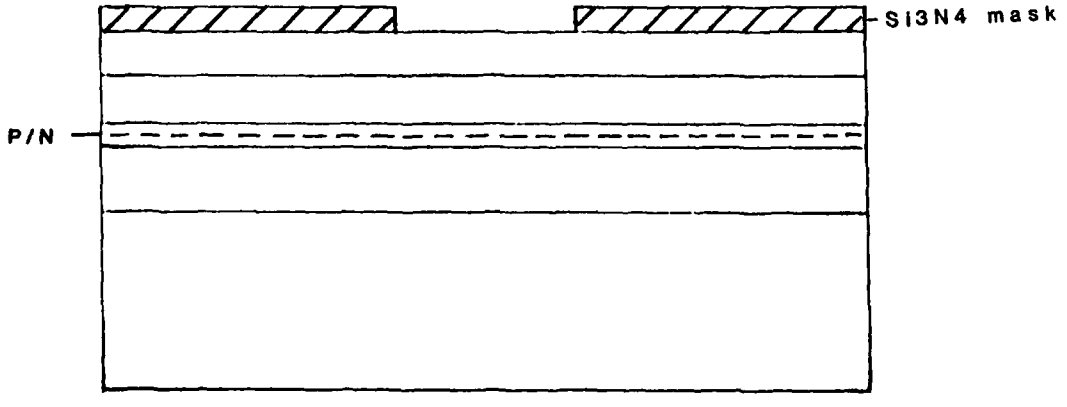

Fig 8f Photo resist Strip

Zn diffusion

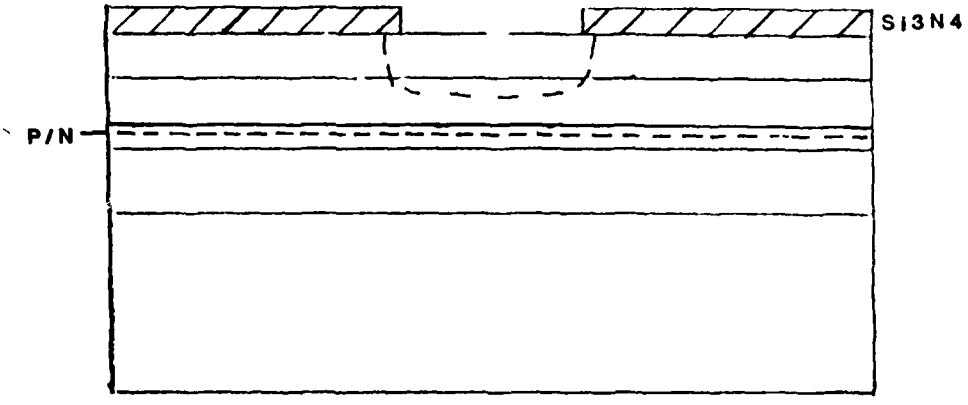

Fig. 8g Selective Zinc Diffusion

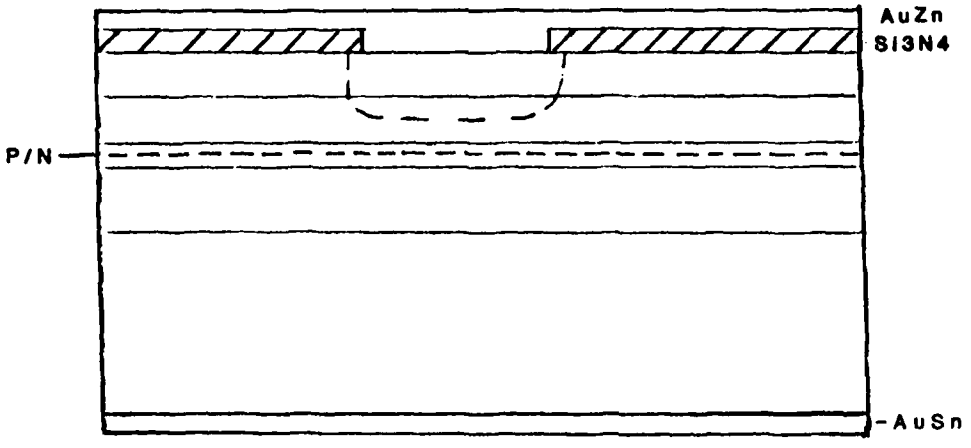

Fig. 8h Evaporation of AuZn-AuSn contacts

4.1 Chemical Vapor Deposition

To form the stripe geometry masking for selective zinc diffusion, a silicon nitride (Si_3N_4) mask, 800 Å thick, must be deposited onto the GaInAsP/InP epitaxial wafer as shown in Figure 8b. The micro-processor controlled CVD system has the capability of depositing both silicon nitride (Si_3N_4) and silicon oxide (SiO_2) films; these films are deposited at 600°C by a gaseous reaction of silane (SiH_4), ammonia (NH_3), and oxygen (O_2) by direct thermal activation in a nitrogen (N_2) carrier gas. A SiH_4/NH_3 ratio of 1:5 results in a deposition rate of ∿40Å/minute.

4.2 Photolithography

The method used to form stripe geometry patterns in quaternary wafers is the standard photolithographic technique also used for processing GaAlAs LED's and CW laser diodes.

In this procedure, positive photo resist (Hunt Chemical Corp. HPR204) is spun onto the GaInsP/InP wafer at 4,000 RPM for 40 seconds, yielding a film thickness of 5,000 Å. The coated wafer is baked for 20 Min. at 120°C prior to exposure to ultraviolet light in the K & S mask aligner.

The exposed wafer is developed with Hunt Corp. L.S.I. developer and a post bake (120°C) anneals the resist. Plasma etching is employed to open diffusion windows in the Si_3N_4 film. The steps described here correspond to Figures 8c thru 8e. The resist is then stripped off, leaving a Si_3N_4 diffusion mask with 3 mil windows as shown in Figures 8f.

4.3 Plasma Etch

To open 3 mil windows in the silicon nitride film and expose the InGaAsP quaternary cap layer, an LFE Corp. Plasma Asher Model #PDS-302 is employed.

The processed InGaAsP/InP structure is placed into the quartz boat in a vertical position and loaded into the Asher's reaction chamber. The chamber is sealed to an atmospheric pressure of 1.0 Torr; the etch gas mixture enters the reaction chamber at 50 cc/min. and is ignited by RF power of 200 watts at a temperature of 175°C. The Si_3N_4 film is selectively etched for 2 minutes at a rate of 425 Å/Min. Once the cycle is completed, the wafer is removed and the photoresist stripped leaving the Si_3N_4 masked GaInAsP/InP wafer ready for selective Zn diffusion as shown in Figure 8f.

4.4 Zinc Diffusion

The Zinc diffusion process as applied here is a 550°C vapor phase semi-sealed ampoule diffusion. The source used in this process is ZnP_2 (200mg), which is loaded into a quartz diffusion boat along with the prepared epi wafer. This in turn is loaded into an open end ampoule. The diffusion tube is then sealed and allowed to purge for a half hour in forming gas ($20\%H_2, 80\%N_2$) at a rate of 5 cfh. Once purged, the gas rate is decreased to 4 cfh and the open end ampoule pushed up flush with the ampoule sealing ball joint. The semi-sealed diffusion system is shown schematically in Figure 9.

Once the seal is made, the 3 zone furnace is pulled over the diffusion boat, centering it in the flat zone of the furnace. The sealed ampoule remains in the furnace for the appropriate length of time necessary to yield the required diffusion depth and concentration.

Figure 10 shows the relationship between junction depth and diffusion time for a 200 mg. ZnP_2 source at 550°C.

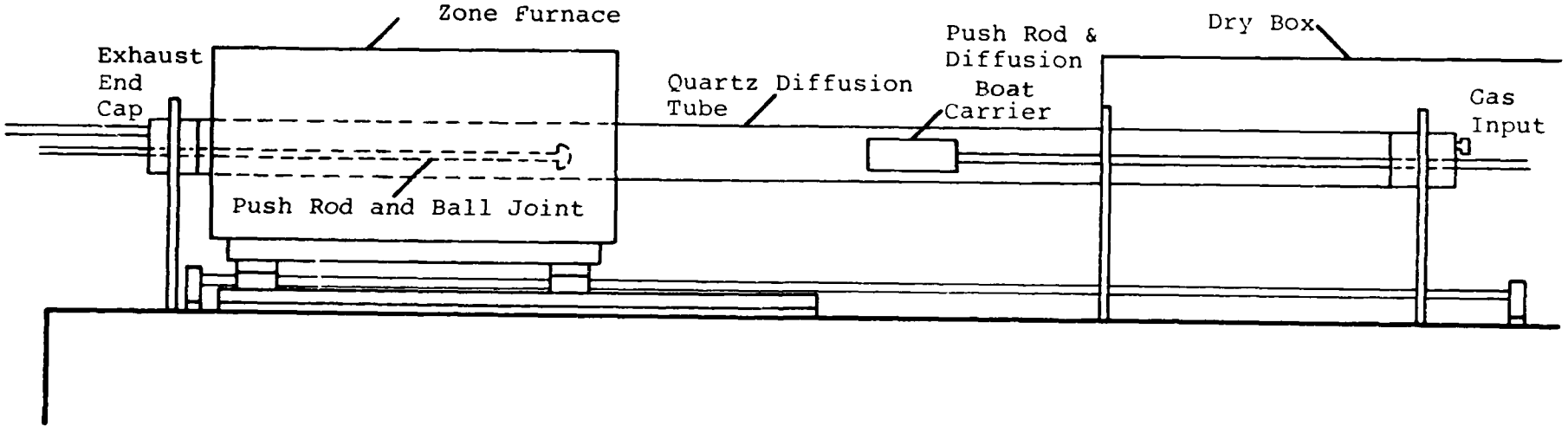

Figure 9. Diagram of Semi-sealed Ampoule Diffusion Apparatus

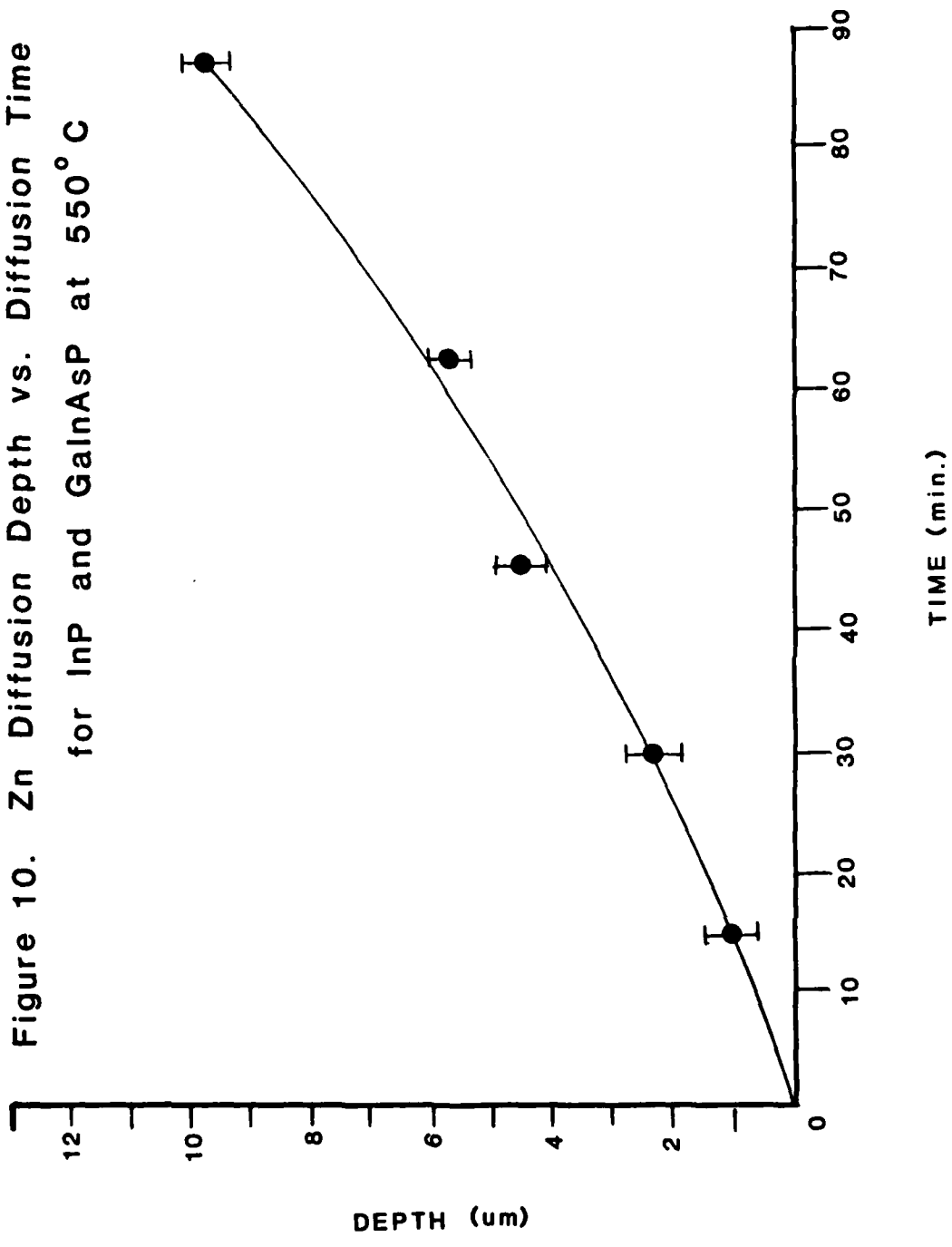

Figure 10. Zn Diffusion Depth vs. Diffusion Time for InP and GaInAsP at 550°C

Once the diffusion has taken place, the ampoule is unsealed while still in the flat zone. This prevents any vapor condensation on the surface of the wafer. The furnace is then rolled back and the sample is allowed to cool to room temperature and removed from the system.

Samples are then cleaved and etched in order to delineate the diffused junction. The etch used is a 1:1 mixture of concentrated nitric acid and D.I. H_2O. to which has been added a suitable source of free Fe^{1+} ions; this etch solution forms a thin oxide film on the n-type material but has no effect on p-type material. Figures 11a, b, and c demonstrate broad area diffusion in InP, selective diffusion in InP, and a selectively diffused quaternary epi wafer.

4.5 AuZn, AuSn Contact Metallization

Following diffusion, the processed wafer is backlapped to 3.5 mils, cleaned in organic solvents and rinsed in alcohol.

Once the wafer is cleaned, it is loaded into the vacuum deposition system, which is then evacuated to less than 10^{-6}Torr; the slice is heat treated to 250°C for 10 min. in order to drive off any remaining surface contamination. Metal evaporation is carried out, depositing 2000 Å of AuSn (95% Au, 5% Sn) on the n-side.

Figure 11. Zn Diffusion in InP

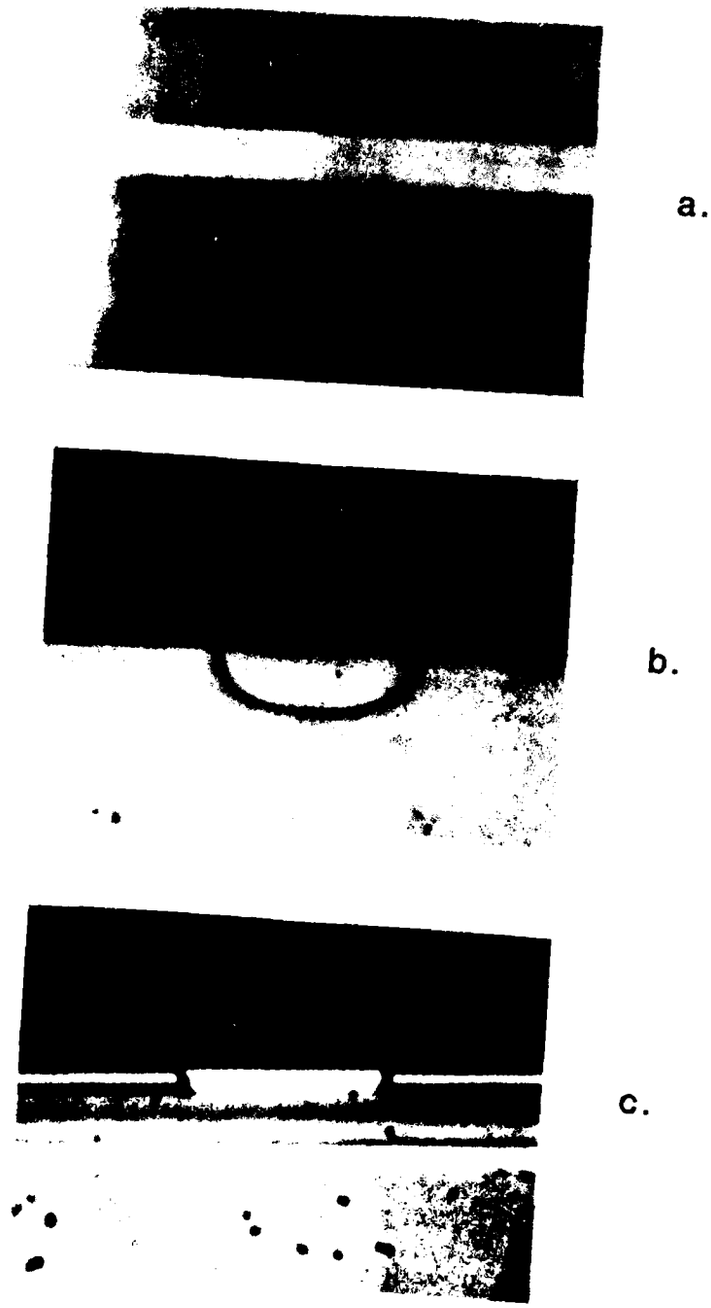

This step is repeated on the P-side of the wafer using AuZn (95% Au, 5% Zn). The contacts are heat treated at 340°C in H_2 for 60 seconds to anneal the ohmic contacts on both n-and p-sides.

4.6 Device Fabrication

After the quaternary epi wafer is metallized, it is cleaved into bars 200 μm wide by approximately 1.0 centimeter long. The cleaved bars are then scribed into individual chips with the 3 mil wide stripe contact centered on the p-side of the chip. The individual laser chips are pulse probed to measure I_{th} and sorted accordingly. For the 75 μm wide by 200 μm long laser cavity, typical pulsed threshold currents for the Type I LOC range from 0.5A to 2.0A at 1.16 μm. The chips are normally bonded with indium p-side up on copper TO-5 headers for evaluation testing. High duty cycle operation (1 to 10%) requires p-side down mounting, however, for reduced chip to case thermal impedance.

5.0 Fiber Coupling Technique

Of primary importance, maximization of launched power received considerable attention during the second and third quarters of the program. The fiber used in all experiments was ITT graded index 55 μm core X 125 μm O.D. communications grade fiber (G202) as specified by NVL. Several techniques were investigated including tapered fiber, epoxy lensing, flame lensing, and a taper/lens combination. When compared to butt coupling, the best method was the taper/lens technique since it permits the lens diameter to be adjusted to match the source size. Optimum coupling was obtained when the lens O.D. was approximately equal to the linear source size. The taper/lens technique is straightforward, requiring a simple drawing apparatus, oxyacetylene microtorch, and fiber cleaving tool. The bare fiber is suspended vertically with a small weight attached to one end and the torch flame passed slowly across the fiber in the horizontal plane. Proper adjustment of the flame, fiber position, and weight, results in highly reproducible stretching of the fiber.

By cleaving the fiber at the appropriate point, one can obtain a cross-section having the same diameter as the laser source width. A spherical lens is formed by flame polishing the cleaved tapered fiber end. For the 75 μm laser source, coupling efficiency in excess of 35% was routinely obtained provided active alignment of the fiber to the laser was utilized. This compares with ∿ 20% for simple butt coupling. (Launch efficiency greater than 75% has been achieved for 5 μm stripe geometry sources with taper lensed fiber). Figure 12a is a photomicrograph of cleaved versus taper/lensed fiber ends. Figure 12b shows a side view of the taper/lensed graded index fiber used for 75 μm stripe laser coupling experiments. Note the slight degree of taper required to obtain the 75 μm diameter lens.

The fiber drawing apparatus used to fabricate the taper/lens combination is shown in the photograph of Figure 13a.

Figure 13b is a photograph ofthe active alignment apparatus used to precisely position the taper/lensed pigtail at the optimum coupling position. The laser is mounted on a stepping motor controlled X-Y stage

Figure 12. Taper/Lensed Fiber Ends

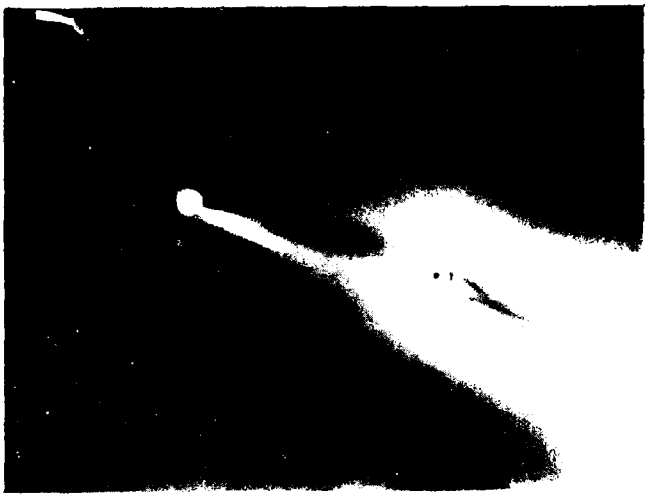

a.

b.

Figure 13. Fiber Drawing, Lensing, and Alignment Equipment

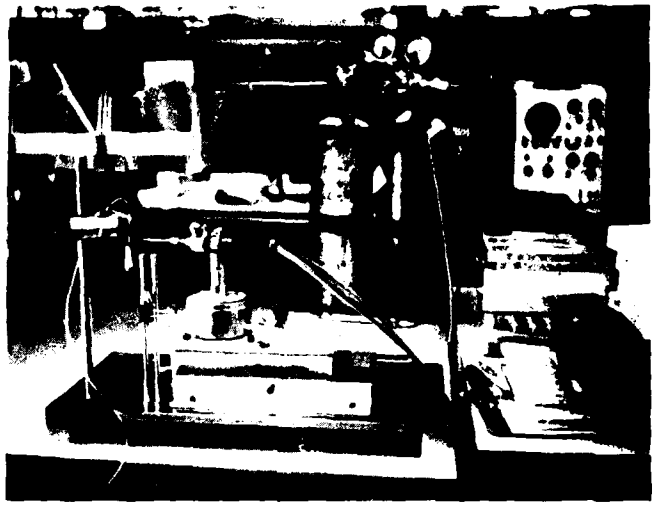

a.

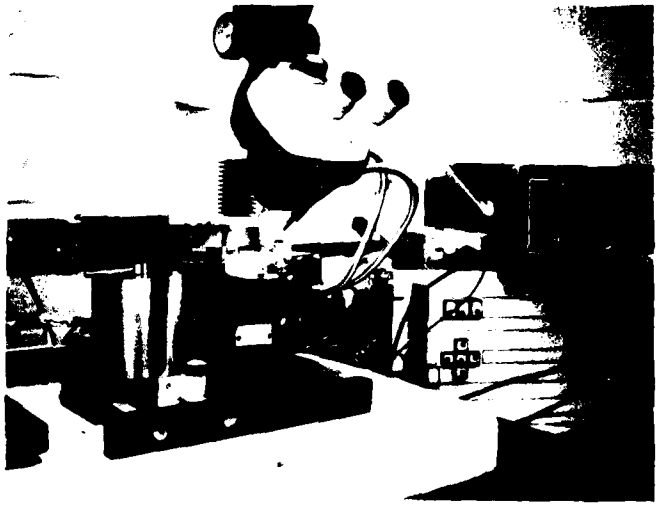

b.

(Micro Control Corp.) which has a 0.1 micron step resolution. The fiber pigtail, embedded in a rigid stainless steel micro-tube, is held in the Z-axis manipulator. The laser is operated under pulsed conditions and the output end of the pigtail coupled to a Germanium PIN photodiode (Optitron). Both drive current and photodiode current pulse are displayed simultaneously on an oscilloscope. The X, Y, and Z stepping motors are jogged until the photodiode output trace is peaked on the scope; the stainless ferrule tube is then attached to the laser package using filled epoxy. Figures 14a and b, optical micrographs of the completed laser package, show the ferrule tube bonded to the TO-5F coax header after alignment to the laser chip. The taper/lensed fiber and is clearly visible in Figure 14b and the reflection of the lens can be observed on the laser front facet.

The key points to be noted with respect to this technique are as follows:

1. The taper-lensed fiber end increases the effective numerical aperture of the fiber and permits the lens diameter to be accurately adjusted to match the laser stripe width.

Figure 14. Fiber Coupled Laser Package

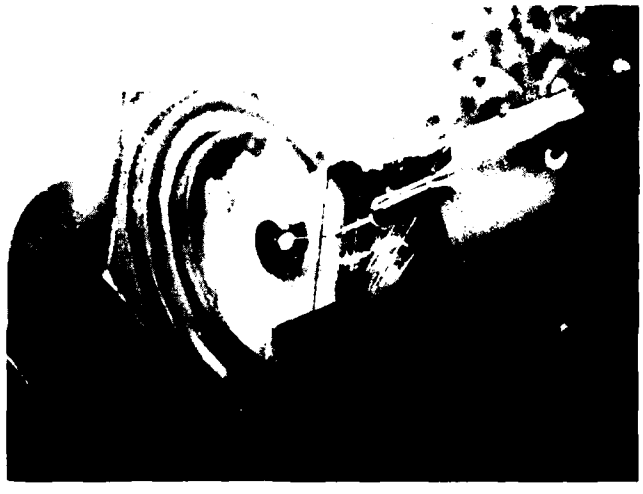

a.

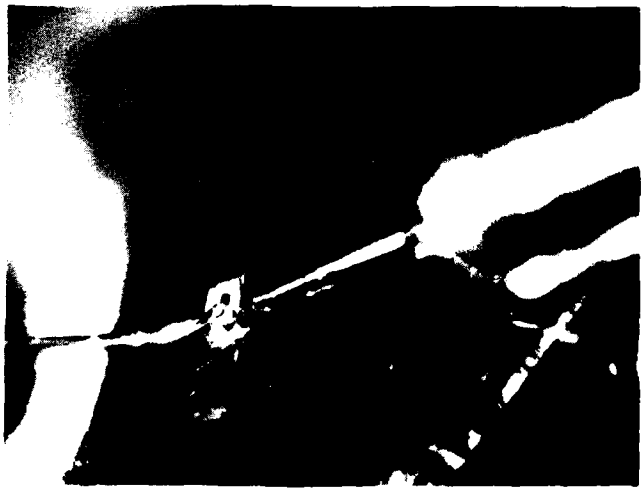

b.

2. Active alignment of the fiber pigtail permits absolute maximization of coupling efficiency for each diode-lens combination.
3. Rigidization of the fiber and using the ferrule tube allows the fiber to be manipulated and affixed to the header without introducing torsion or bending stress on the fiber.
4. The use of fast curing filled epoxy eliminates degraded coupling efficiency due to shrinkage. This technique has demonstrated excellent long-term stability; fiber coupled diodes stored for 6 months in the normal lab ambient showed no measurable change in optical output power.

6.0 Longwave Quaternary LOC Performance Characteristics

The histogram in Figure 15 shows the distribution in pulsed threshold current, I_{th} for 55 randomly selected chips from quaternary LOC wafer RQ 111. Exceptionally high yield is characteristic of wide cavity LOC structures provided the P/N junction is accurately located within the active layer. Only 7% of the chips were non-lasers with the peak in the distribution around 1200 mA. Devices delivered under this contract were fabricated from chips having 800-1000 mA thresholds. The average threshold current density assuming a diode area of 75 μm by 200 μm, is 8.5KA/cm^2 for the 0.45 μm wide cavity at λp = 1.16 μm. The J_{th}/μm is roughly 3 times greater than for comparable GaAlAs ternary structures suggesting less effective carrier confinement in the quaternary.

Peak wavelength, threshold current, and total output power measurements are given in Figure 16 for the devices delivered under this contract. Power output was measured at low duty factor (1KHz, 50 nsec) using a 1 millimeter diameter calibrated Ge PIN photodiode (Rofin GE7460). The spectral responsivity curve for this diode is given in Figure 17. Calibration was

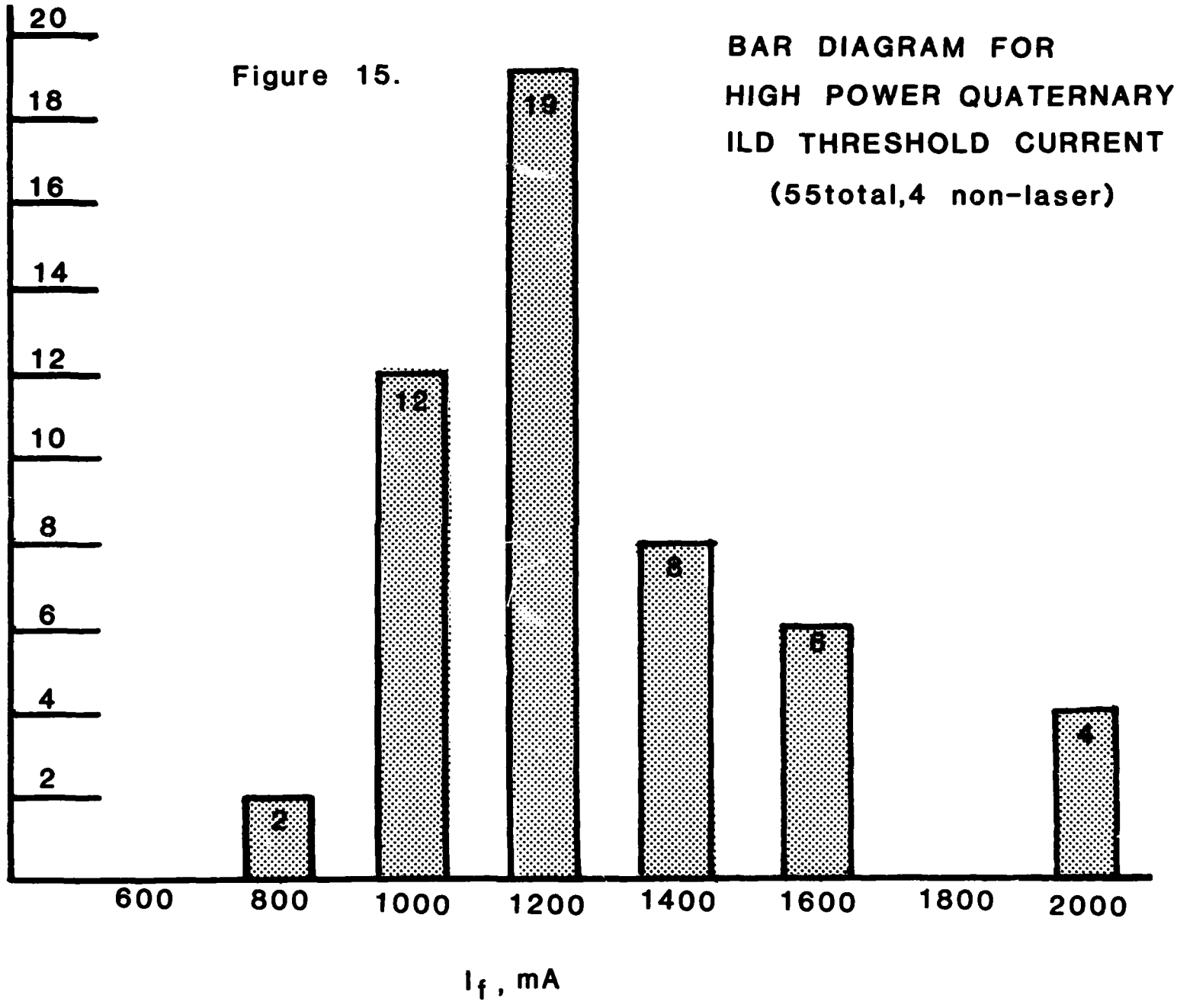

Figure 15.

BAR DIAGRAM FOR
HIGH POWER QUATERNARY
ILD THRESHOLD CURRENT
(55total,4 non-laser)

Lot:
RQ-111

Test Conditions:
1KH$_z$, 50 nsec
Case Negative!

Detector Calibration:
1.50 mW/mV @ 1.15 μm
(GE 7460)

#	I_{th}, Amps	I_f (max), Amps	V_{det}, mV	P_o (max), mW	λ_p, μm
B-25	0.9	2.25	180	270	1.16
B-26	0.9	2.25	250	375	1.16
B-28	0.9	2.25	180	270	1.16
B-31	0.9	2.25	220	330	1.16
B-32	0.8	2.00	210	315	1.16
B-35	0.9	2.25	200	300	1.16
B-37	1.0	2.50	250	375	1.16
B-38	1.0	2.50	210	315	1.16
B-41	1.0	2.50	180	270	1.16
B-48	0.9	2.25	210	315	1.16
				*	
F-1	1.0	2.00	23	35	1.16
F-2	0.9	2.00	55	83	1.16
F-4	1.0	2.00	31	47	1.16
INSP. BY					

Figure 16. Quaternary LOC Power Output Data

*P_o from 55 μm core GI fiber pigtail (ITT-G202).

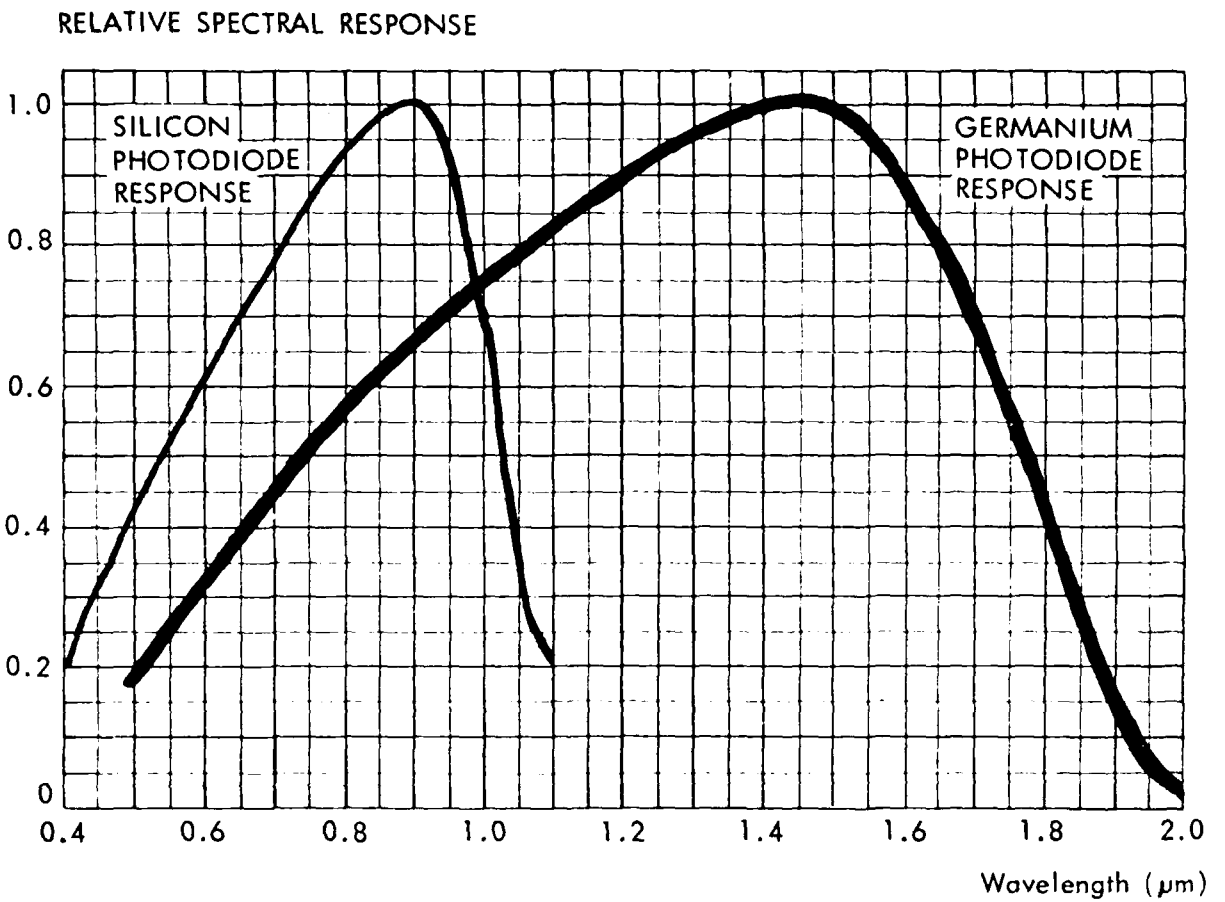

Figure 17. Spectral Responsivity Curve for Germanium PIN Photodiode

accomplished using GaAs (904 nm) diodes of known power as determined with an NBS traceable ITT F4000 vacuum photodetector. These lasers had a far field distribution similar to that of the longwave quaternary lasers so that power collection was the same for both types. By measuring the GaAs diodes with the Ge detector and using the spectral responsivity curve, a calibration factor of 1.50 mW/mV at λp = 1.15 μm was determined. Several hundred milliwatts total output was reliably achieved and the average differential efficiency (DQE) was 0.23 mW/mA per facet for the 10 lasers delivered without fibers. Although the delivered diodes were conservatively rated at only 2.5 X I_{th} or slightly greater than 4 mW/μm of active junction length, about twice this power level can be achieved before one begins to observe the onset of catastrophic damage.

Figure 18 shows a typical output spectrum from the quaternary LOC with the output peak located at 1.16 μm and the spectral half width of 7 nm. Figure 19 is a higher resolution spectrum measured from a device with a pigtail. Finally, Figure 20 shows the far field perpendicular beam divergence typically observed for these devices. The 45° FWHM divergence

Figure 18. TYPICAL LASING SPECTRUM FOR HIGH POWER QUATERNARY ILD

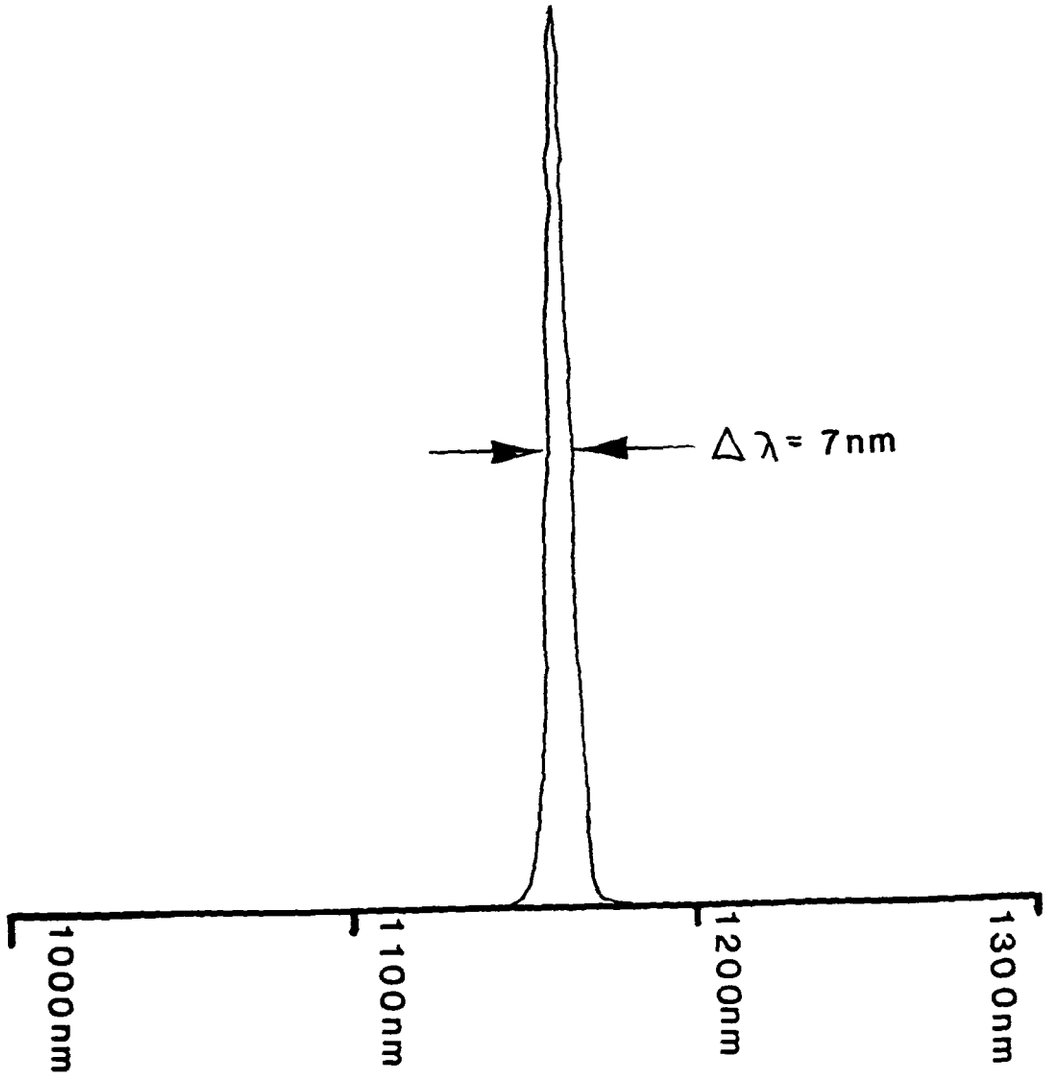

RQ 111-B
PRF 1KHz
PW 120nsec
I_f 2.2A

Figure 19.

TYPICAL LASING SPECTRUM FOR FIBER COUPLED HIGH POWER QUATERNARY ILD

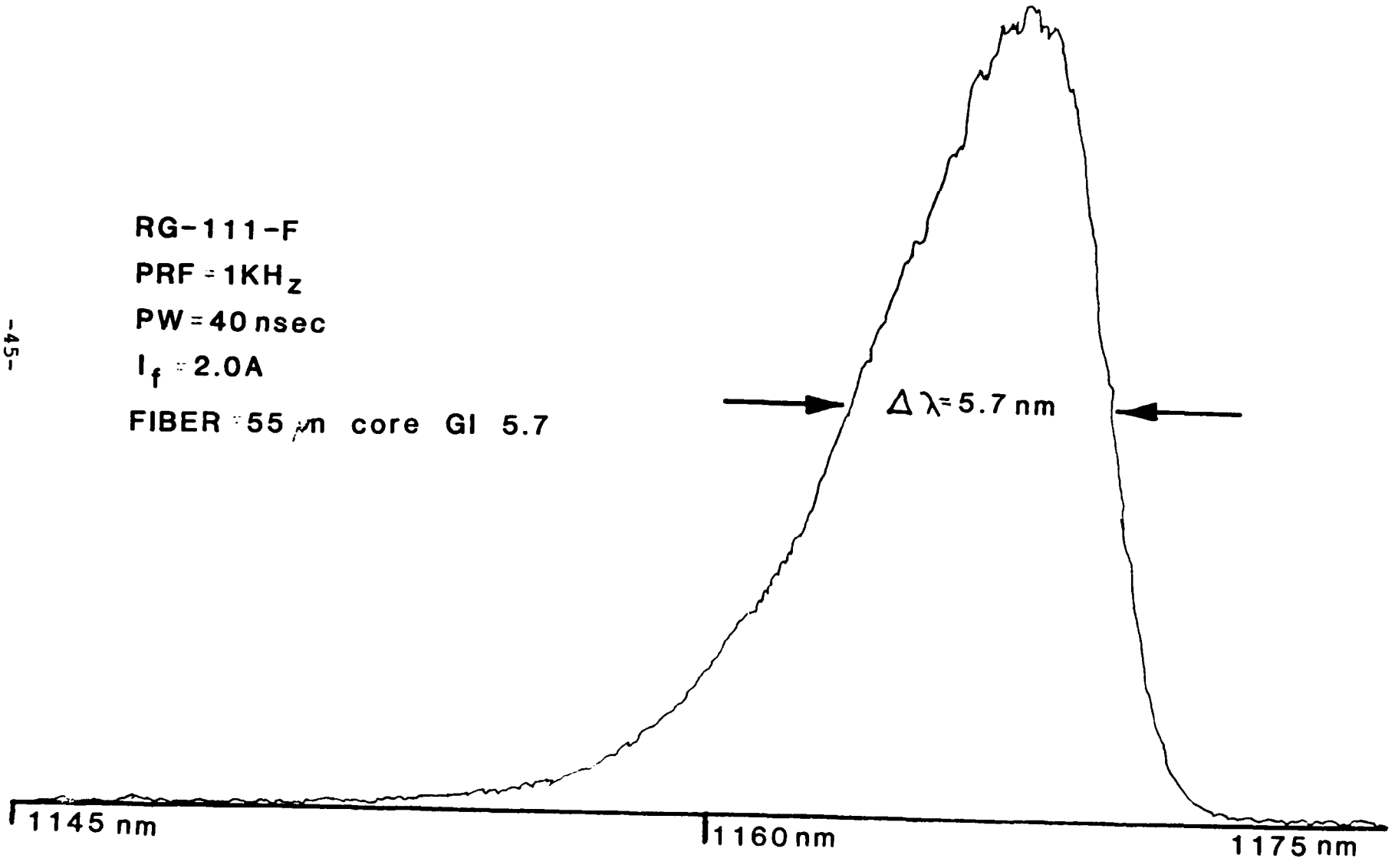

Figure 20.

PERPENDICULAR BEAM DIVERGENCE FOR HIGH POWER QUATERNARY ILD

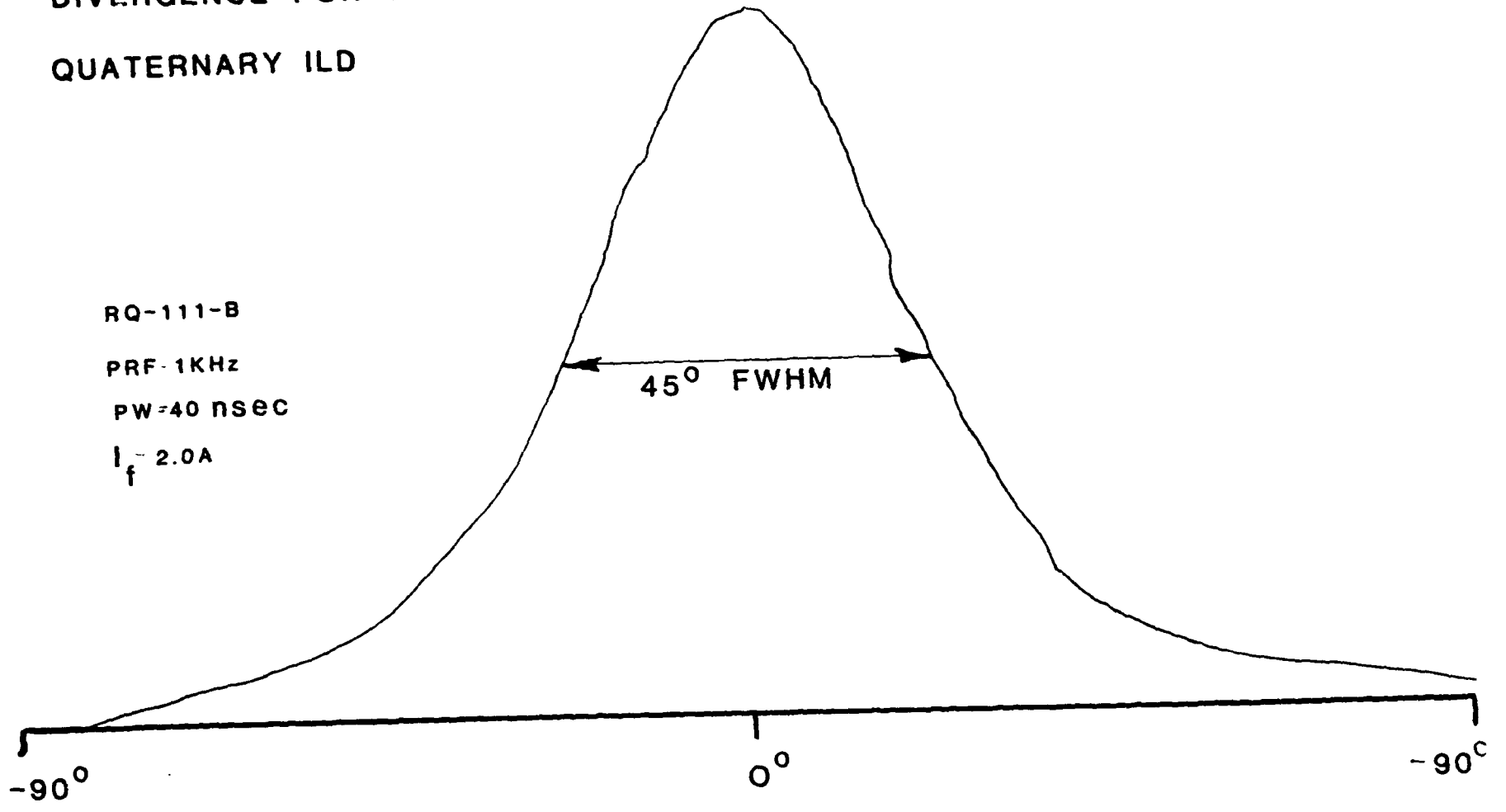

indicates a fairly high degree of optical confinement for the 0.45 μm cavity width device. This can be reduced by making the active region much wider but with a severe penalty in threshold current.

Improved performance for fiber coupled devices could be achieved by further reduction of the stripe width accompanied by a corresponding increase in active region thickness. This would provide a more suitable match to 50 μm core fiber and reduce the beam divergence , while maintaining roughly the same threshold and DQE as for the prototype devices demonstrated during the course of this program.

7.0 Summary and Conclusion

Excellent peak power performance has been achieved in fiber coupled stripe geometry quaternary LOC laser diodes at 1.16 μm. Since the recent publication by Itaya et al (Tokyo Institute of Technology) compiling complete composition bandgap data for lattice matched GaInAsP, pulsed laser operation has been extended to 1.04 μm on the low end and 1.42 μm at the longwavelength extreme. Further development of the quaternary LOC structure is required, however, to increase the peak power capability beyond the levels achieved under this contract and at wavelengths in the 1.5 μm region.

Additionally, refinement of growth techniques, ohmic contact formation, design and implementation of suitable optical facet coatings, and extended long term and accelerated life studies are needed to fully maximize power output and reliability of this important device.

DISTRIBUTION LIST

No Copies	Addressee
2	Director, National Security Agency ATTN: R52 Geoff Burge 9800 Savage Road Fort Meade, MD 20755
2	Advisory Group on Electric Devices ATTN: Secretary, Working Group D 201 Varick Street New York, NY 10014
2	Dr Eirug Davies ESO Deputy for Electronic Technology Hanscom AFB Bedford, MS 01731
2	Sirector Code 6570 ATTN: Henry Taylor Naval Research Laboratory Washington, DC 20375
2	Harry Diamond Laboratories ATTN: HD-RT-CD/13300 (Dr Greg Sztankay) 2800 Powder Mill Road (Dr Norm Berg) Adelphi, MD 20783
5	ARPA Defense Service Office ATTN: Dr. Reynolds 1400 Wilson Boulevard Arlington, VA 33309
5	USARO RTDK ATTN: DRXRO-PH Durham, NC
1	Commandant US Army Infantry School Ft Benning, GA 31905
5	Director Defense Advanced Research Projects Agency Rosslyn, VA 22209
1	Commander HQ DARCOM ATTN: DRCCP-E Alexandria, VA 22333
2	Commander, ADS ATTN: XRQI (mr. Barthell) Wright Patterson AFB, OH 45433
2	Director CS&TA Laboratory ATTN: DELCS-AC (Mr. Longinotti) Fort Monmouth, NJ 07703
2	Commander, NTEC PMTRADE ATTN: DRCPM-AP (Major Singer) Orlando, Florida 32813
2	Commander, NTEC PMTRADE ATTN: DRCPM-GS (LTC Slate) Orlando, FL 32813
2	Commander USA CORADCOM CENCOMS ATTN: DRDCO-COM-RM-1 (Mr. L. Coryell) Fort Monmouth, NJ 07703
2	Ted Kostink Code 605 NASA Godard Space Flight Center Greenbelt, MD 20771
12	Defense Documentation Ctr ATTN: DDC-TCA Cameron Station (Bldg 5) Alexandria, VA 22314
1	NASA Scientific & Tech Info Facility ATTN: Acquisitions Branch (S-AK/DL) P.O. Box 33 College Park, MD 20740
1	Study Center National Maritime Research Ctr King's Point, NY 11024

DISTRIBUTION LIST

No Copies	Addressee
1	Commander ERADCOM ATTN: DRDEL-AP-OA M. Geisler Adelphi, MD 20783
2	Director CS&TA Laboratory ATTN: DELCS-D Fort Monmouth, NJ 07703
2	Director Electronics Technology & devices Lab ATTN: DELET-D Fort Monmouth, NJ 07703
2	Director Signal Warfare Lab ATTN: DELSW-D Vint Hill Station VA 22186
1	Department of Defense Production Engineering Spt Ofc (PESO) ATTN: D. Anderson Cameron Station Alexandria, VA 22314
1	Commander Naval Electronics Lab Ctr ATTN: Library San [illegible], CA 92152
3	Commander AFSC/ACC Andrews AFB, MD 20334
1	Dept of Defense Production Engineering Spt Ofc (PESO) ATTN: H.K. MacKechnie Cameron Station Alexandria, VA 22314

No Copies	ADDRESSEE
2	Director Atmospheric Sciences Lab ATTN: DELAS-D White Sands Missile Range, NM 88002
2	Director Electronic Warfare Lab ATTN: DELEW-D Fort Monmouth, NJ 07703
2	Commander Harry Diamond Labs ATTN: DELHD-AC Adelphi, MD 20783
3	Commander CERCOM ATTN: DRSEL-CP-CR Fort Monmouth, NJ 07703
3	Commander ESD/ACC Hanscomb AFB, MA 01730
1	Commander US Naval Ordnance Lab/White Oak ATTN: Technical Library Silver Spring, MD 20910
1	Armament Development & Test Ctr ATTN: DLOSL, Tech Library Eglin Air Force Base, FL 32542
20	Director NVGEOL ATTN: DELNV-L (Skeldon) Fort Belvoir, VA 22060

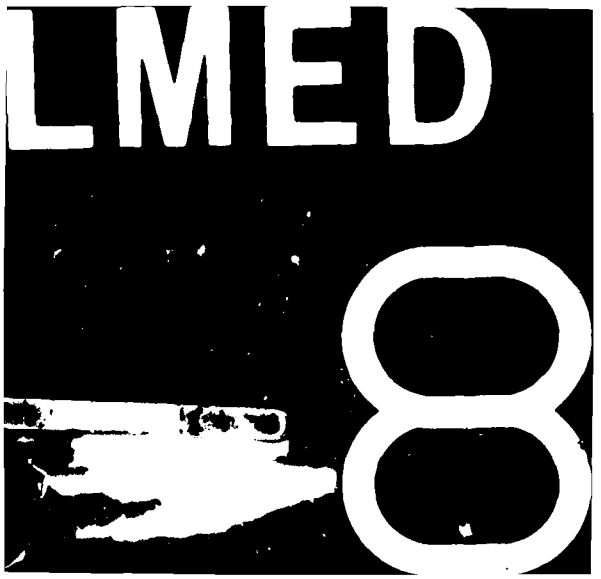
LMED
8